

O

AR-007-998

DSTO-TN-0024

T

A Comparison of Digital and
Analogue Vibration Analysis
Techniques for the Detection of
Ball Bearing Faults

Mark Shilo

S

APPROVED FOR PUBLIC RELEASE

© Commonwealth of Australia

D

A Comparison of Digital and Analogue Vibration Analysis Techniques for the Detection of Ball Bearing Faults

Mark Shilo

**Airframes and Engines Division
Aeronautical and Maritime Research Laboratory**

DSTO-TN-0024

ABSTRACT

A comparison of Digital and Analogue Envelope Detection techniques was performed on the vibration signals generated by the failure of three NSK type 7006C angular contact bearings to determine the relative merits of each technique.

RELEASE LIMITATION

Approved for public release

DEPARTMENT OF DEFENCE

DEFENCE SCIENCE AND TECHNOLOGY ORGANISATION

19960806 040

Published by

*DSTO Aeronautical and Maritime Research Laboratory
PO Box 4331
Melbourne Victoria 3001*

*Telephone: (03) 9626 8111
Fax: (03) 9626 8999
© Commonwealth of Australia 1995
AR No. AR-007-998
January 1996*

APPROVED FOR PUBLIC RELEASE

A Comparison of Digital and Analogue Vibration Analysis Techniques for the Detection of Ball Bearing Faults

Executive Summary

'Envelope Detection' is a technique of using vibration analysis for detecting the presence of surface defect faults in ball bearings and rolling element bearings. Envelope detection has been demonstrated to be capable of detecting ball bearing faults where traditional vibration analysis techniques have been unsuccessful. There are many tools commercially available for bearing fault detection, some of which use the technique of envelope detection. Personal computers (PCs) are used extensively for all kinds of vibration analysis including envelope detection, and the question has arisen as to how the efficiency of the digital methods employed in computers compares with that of analogue methods used by commercial tools in detecting ball bearing faults.

The Bruel and Kjaer analogue envelope detector WB1048 was chosen for a comparison with a PC-based digital envelope detection algorithm, and three test specimen ball bearings were used to gauge the performance of the two fault detection techniques. The brand-new, fault free test specimens were driven at high speed under high load while their vibration signatures were recorded, until surface defect faults developed naturally. Analysis of the vibration recordings with both digital and analogue envelope detection techniques showed that both methods were able to detect the onset of the naturally occurring fault at the same point in the vibration recordings, but the analogue device provided results more quickly than the digital technique, due to computation time needed for the digital technique. However, the digital technique offers other advantages that the analogue device cannot, such as readily linking with a database, and other PC-based condition monitoring and trending programs. Early detection of bearing faults using such vibration analysis methods as envelope detection will enable operators of rotating machinery to extend the service life of many types of equipment.

Contents

LIST OF FIGURES

NOTATION

1. INTRODUCTION.....	1
2. THEORETICAL BACKGROUND	1
2.1 Analogue Envelope Detection	2
2.2 Digital Envelope Detection.....	3
3. APPARATUS	4
3.1 Test Specimen.....	4
3.2 Test Equipment.....	5
3.3 Rig Instrumentation and Data Analysis Equipment	7
4. TEST RESULTS.....	7
4.1 Test 1.....	7
4.2 Test 2.....	8
4.3 Test 3.....	9
5. RESULTS AND DISCUSSION	10
6. CONCLUSIONS.....	16
7. REFERENCES	17
8. ACKNOWLEDGMENTS	17
APPENDIX A.....	18
APPENDIX B.	19

LIST OF FIGURES

1. The raw vibration signal	2
2. Vibration signal band pass filtered about the resonance peaks	2
3. Fourier Transform of the rectified signal reveals the fundamental fault frequency	2
4. Frequency shift the vibration signal	3
5. Isolate the resonance and envelope the corresponding time signal	3
6. Enveloped time signal, and corresponding FFT showing fundamental fault frequency	4
7. Relevant bearing dimensions	5
8. Schematic diagram of Bearing Test Rig	6
9. Photograph of Bearing Test Rig	6
10. a) Dissassembled NSK 7006C angular contact bearing	12
b) Outer Race failure	12
11. a) Raw results	14
b) Standardised Results	14
12. Progression of bearing failure of tests 1, 2, and 3	15
B1. Envelope Detector connector plug pin functions	20
B2. Battery supply and input/output circuit for Envelope Detector	21

NOTATION

BR	Ball rolling frequency
CAGE	Cage frequency
d_B	Ball diameter
d_i	Inner race diameter
d_p	Pitch diameter - $d_p = d_B + d_i$
FFT	Fast Fourier Transform
f_i	Inner race frequency
IRBP	Inner race ball pass frequency
N	Number of balls
ORBP	Outer race ball pass frequency
θ	Bearing contact angle

SUBSCRIPTS

B	Ball
i	Inner race
P	Pitch diameter
ω	Frequency

1. INTRODUCTION

Bearings, both journal and rolling element, provide a vital function in the operation of all types of rotating machinery, giving low friction support for both axial and radial loads on rotating shafts. Damaged bearings may cause failure of larger and more expensive components in a machine, resulting in costly down-time and repairs that may have been avoided if the bearings were replaced before significant damage had occurred.

Bearing fault detection has been achieved by the monitoring of oil temperature, detection of oil borne metallic debris, and more recently by a variety of vibration monitoring techniques. Simple vibration analysis techniques such as RMS level and spectral analysis can detect known failures in simple machines, but often the initial indications that a fault is developing in a more complex machine or plant are indistinguishable from the high level of background vibrations from other machine components, or even other machines.

Envelope detection is a method of bearing fault detection that enables bearing fault frequencies to be enhanced and so be more easily detected at the early stages of fault development. Traditionally this has been accomplished with analogue circuitry, but the increasing use of digital signal processing has led to the development of digital envelope detection methods. This report compares the relative merits of digital and analogue envelope detection techniques and makes a recommendation for the future use of these methods. Three NSK type 7006C angular contact ball bearings were failed by extended operation at high loading, and the vibration signals were recorded for subsequent analysis using both digital and analogue envelope detection techniques.

2. THEORETICAL BACKGROUND

The analysis of the vibration recordings was performed using both digital and analogue envelope detection vibration analysis techniques. A description and explanation of the mechanisms of these methods is provided as follows.

Envelope detection is a method of identifying and isolating modulation frequencies in a vibration signal which may have been generated by impulses arising from a damaged component. The actual frequency of the impulses is often concealed in the spectrum by the noise and frequency components generated by other machine components, but the sharp nature of the fault impacts causes the machine structure to ring at its resonant frequencies. This condition is observed as an increase in amplitude of the portion of the vibration spectrum corresponding to the resonant frequencies. It is found that sidebands of the original impulse frequency are contained in the elevated area of the spectrum, generating the observed modulation frequency.

2.1 Analogue Envelope Detection

Envelope detection may be achieved by the use of electronic filters and rectifiers which act upon the pure analogue signal to extract the modulation frequencies. Unlike digital envelope detection which requires the conversion of the analogue signal to digital format, the analogue method permits real-time analysis of an operating machine. The processes that are performed by the analogue equipment are as follows:

1. The vibration signal is band pass filtered at a user-specified position on the spectrum, as shown in figures 1 and 2.

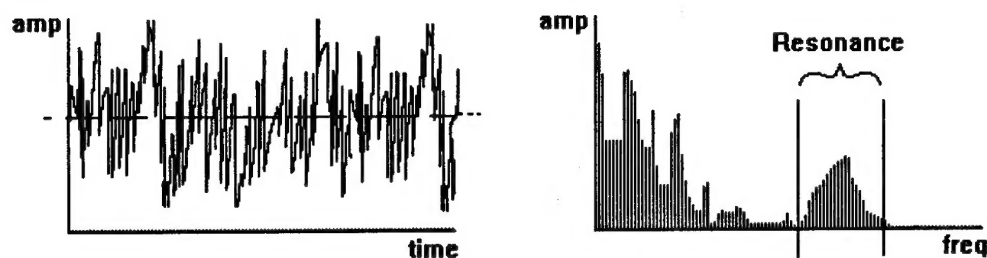


Figure 1. The raw vibration signal.

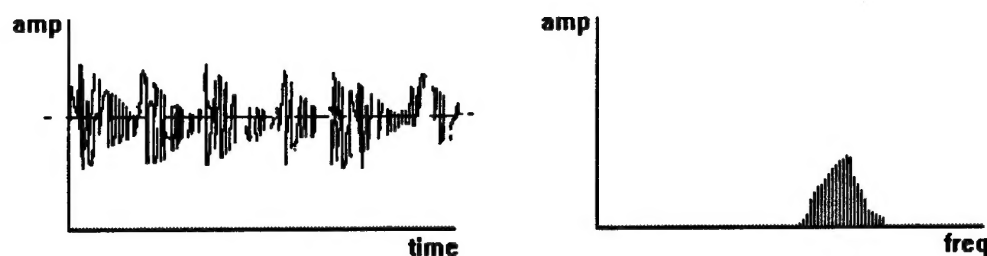


Figure 2. Vibration signal band pass filtered about the resonance peaks.

2. The resultant time signature is rectified with a full wave rectifier, which produces a fundamental fault frequency for a damaged bearing. The theoretical mechanism for fault frequency detection is outlined in detail in Appendix A. Figure 3 shows the resulting fault frequency.

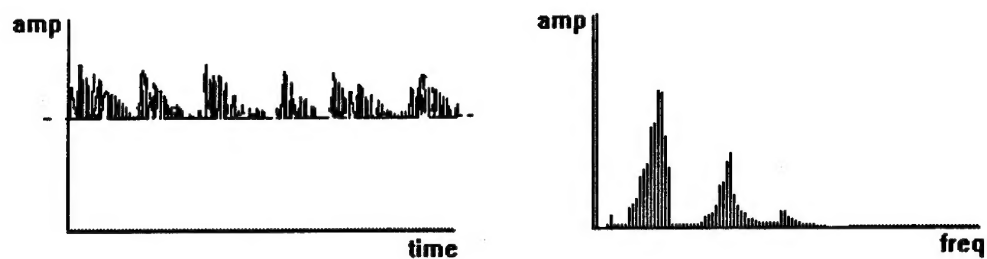


Figure 3. The Fourier Transform of the rectified signal reveals the fundamental fault frequency.

The resultant spectrum showing the modulation frequency is displayed continuously on the spectrum analyser with an update rate that is dependent only upon the processing speed of the spectrum analyser.

2.2 Digital Envelope Detection

It is possible to extract modulation frequencies from the vibration spectrum through computation algorithms that may be performed on a Personal Computer after the analogue vibration signal is digitised and stored in computer memory with the use of an Analogue-to-Digital converter. The envelope detection algorithms used here were developed at AMRL and programmed in Pascal on a Terran T30 IBM PC, and involve the following procedures:

1. Capture a specified interval of vibration signal at a user-defined acquisition rate.
2. Compute the frequency spectrum using an FFT algorithm, thus enabling the resonance peaks to be identified.
3. Frequency shift the signal by multiplying by a complex exponential related to the centre frequency. See figure 4.
4. Low pass filter the frequency shifted signal to isolate the modified resonance. See figure 5.
5. Envelope the complex time signal : $|x(t)|^2 = (\text{Re } x(t))^2 + (\text{Im } x(t))^2$
6. Calculating the FFT of the enveloped time signature. See figure 6.

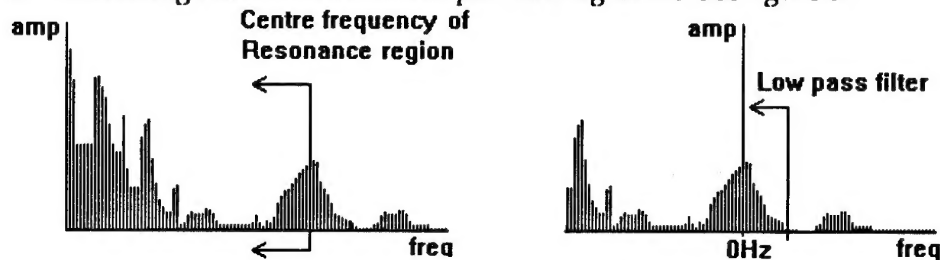


Figure 4. Frequency shift the vibration signal.

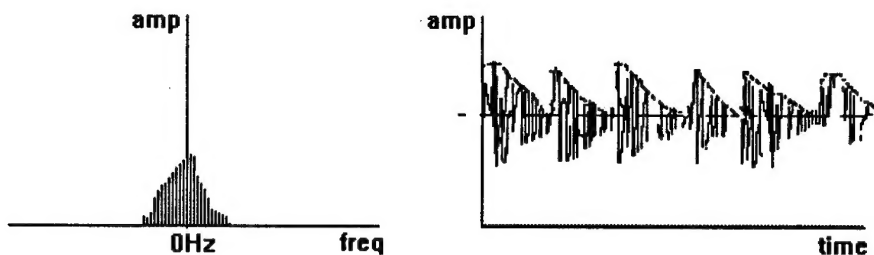


Figure 5. Isolate the resonance and envelope the corresponding time signal.

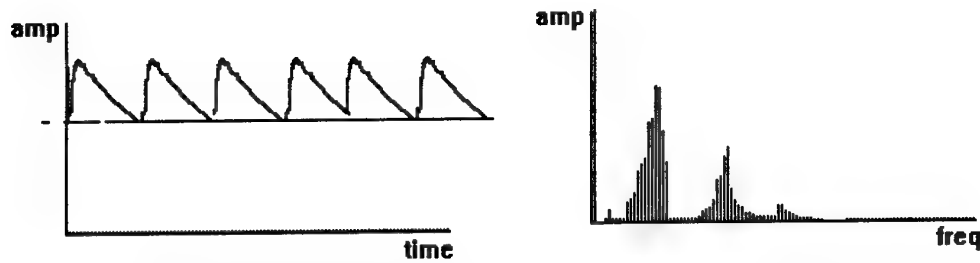


Figure 6. Enveloped time signal, and corresponding FFT showing fundamental fault frequency.

The resultant spectrum contains an enhanced modulation frequency component with harmonics, the amplitude and relative sizes of which are indicative of the severity of the fault.

3. APPARATUS

3.1 Test Specimen

The ball bearing used in the experiments was a NSK type 7006C angular contact bearing, with contact angle $q = 15^\circ$ and the number of rolling elements $N = 14$. A dimensioned diagram of the bearing is shown in figure 7.

The vibration frequencies associated with a particular fault depend on the relative size of the bearing components, the running speed of the bearing, the number of balls in the bearing, and on which bearing component the fault occurs. There are four possible locations for a fault : inner race, outer race, ball, and cage. For these four fault locations, the associated vibration frequencies of a particular fault may be predicted using the following formulae [1], which are based on the assumption that no slippage of bearing components occurs. In practice slippage does occur to a small extent, slightly modifying the calculated values. The formulae shown here are for the case of a fixed outer race and a rotating inner race.

$$ORBP = \frac{N}{2} f_i \left(1 - \frac{d_B}{d_p} \cos\theta \right)$$

$$IRBP = \frac{N}{2} f_i \left(1 + \frac{d_B}{d_p} \cos\theta \right)$$

$$BR = f_i \frac{d_p}{2d_B} \left(1 - \left(\frac{d_B}{d_p} \cos\theta \right)^2 \right)$$

$$CAGE = \frac{f_i}{2} \left(1 - \frac{d_B}{d_p} \cos\theta \right)$$

Where:

ORBP is the outer race ball pass frequency,
 IRBP is the inner race ball pass frequency,
 BR is the ball rolling frequency,
 CAGE is the cage frequency,
 N is the number of rolling elements, which for this bearing is 14 balls,
 dB is the ball diameter,
 and $dP = dB + di$,
 where di is the diameter of the inner race, dP pitch diameter.
 fi is the rotation frequency of the inner race (shaft speed, in this case),
 and q is the angle of contact in the bearing. (See figure 7.)

For an NSK 7006C bearing, with $fi = 100$ Hz, the component frequencies are:

ORBP = 587.0 Hz

IRBP = 814.0 Hz

BR = 291.5 Hz

CAGE = 41.9 Hz.

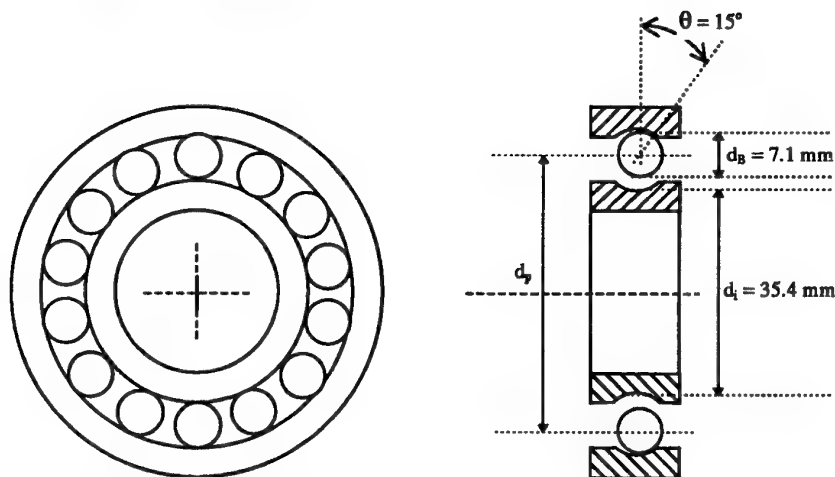


Figure 7. Relevant Bearing Dimensions.

3.2 Test Equipment

The test specimens were loaded axially and driven in the AMRL Bearing Test Rig to induce natural failure. This rig has been used in previous experimental programs [1], and has been slightly modified for each test program. Figure 8 shows a schematic of the Test Rig in its current form. Figure 9 is a photograph of the Bearing Test Rig.

The test specimen is an NSK type 7006C angular contact bearing.

The Rig was driven by a Hebcos 3 Hp, 3 Phase electric motor.

The speed was controlled by a Danfoss Static Frequency Converter, type VLT5, with 3 Phase 38 - 380 Volts at 5 - 50 Hz.

Lubrication and cooling of the test specimen and support bearings were achieved by recirculation of Mobil Jet Oil 2 through a water cooled heat exchanger.

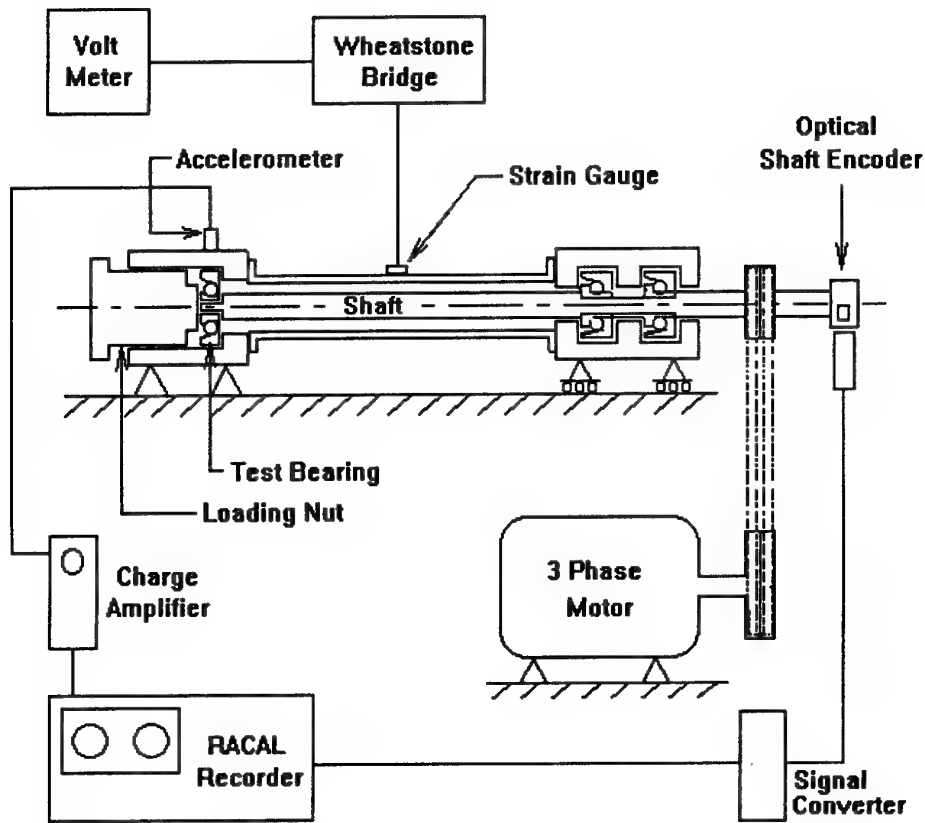


Figure 8. Schematic Diagram of Bearing Test Rig.

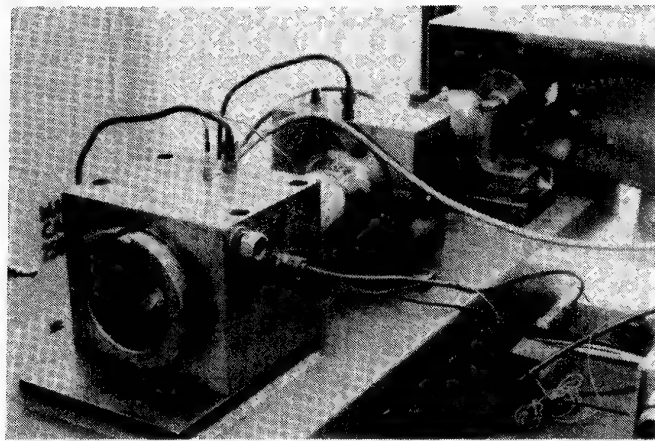


Figure 9. Photograph of the Bearing Test Rig.

3.3 Rig Instrumentation and Data Analysis Equipment

The vibration signal was generated by a single type 303A02 PCB accelerometer, which was then amplified by a model 464A PCB charge amplifier and continuously observed with the aid of an Iwatsu Cathode Ray Oscilloscope, and the RMS level measured with a Keithly 179A TRMS multimeter. The vibration signal was recorded with a ten channel Racal V-store data recorder.

The shaft speed was measured with a Spectral Dynamics optical tachometer and model 13135 GP signal converter, and the shaft speed was monitored by displaying the frequency of the tachometer pulses with a Data Precision type 5845 counter. The tachometer pulse was also recorded on the Racal data recorder.

The temperature of the return oil from the test specimen and the support bearings was measured with two Copper/Constantan thermocouples and displayed on a degrees Celsius voltmeter manufactured by Ether Ltd.

The applied load was measured with a four-element 350 ohm strain gauge bridge with ± 5 volt supply, coupled to a Sanborn type 8875A differential amplifier. The signal was amplified by a factor of 100 and the resulting voltage displayed on a Hewlett Packard 3478A Multimeter.

Post test analysis was performed on the recorded data, with the digital analysis of the vibration records performed on a Terran T30 386 PC, using algorithms developed at the AMRL, while the analogue analysis was performed using the WB1048 envelope detector and the Bruel and Kjaer 2034 Signal Analyser.

The envelope detector that was used in the analysis is a WB1048 Bruel and Kjaer device which has connections designed to operate specifically in conjunction with the model 2515 Bruel and Kjaer signal analyser. Use of the existing model 2034 signal analyser was facilitated by the construction of an interface and power supply circuit at the AMRL. The details of this circuit are provided in Appendix B.

4. TEST RESULTS

4.1 Test 1

The test bearing was run with an initial axial load of 4.5 kN and inner race speed of 100 Hz. Recordings were made periodically with the Racal recorder set up for a tape speed of 30 inches per second on IRI standard wideband two (2), giving a frequency bandwidth of 0 - 100 kHz. After 16.6 hours it was decided to increase the load to 6.6 kN to hasten the onset of failure. The bearing withstood the increased load for a further 12.5 hours without showing any indication of increased vibration, so the load was increased a second time to 9.0 kN. Sudden failure occurred after a total run time of 41.2 hours. The bearing failed on the outer race, showing a distinctive pitting

formation, or spall approximately 3mm by 5mm in area, at one location on the outer race only. The failed bearing is shown in figure 10.

The sudden nature of the initiation and progression of the outer race fault was due to the high loading on the test bearing. This, combined with the fact that the interval between periodic recordings was large and the length of each recording small due to the 100 kHz frequency band width, resulted in a vibration record of the before failure condition, and a vibration record of the after failure condition, but no recorded data of the fault initiation and progression stages.

Subsequent tests used reduced tape speed to enable greater recording time per cassette, while reducing the frequency bandwidth.

Summary of Test 1.

Inner Race speed : 100 Hz ; tape recording frequency range : 0 - 100 kHz

Outer Race Ball Pass fault frequency : measured at 595.7 Hz.

Note: The theoretical bearing frequencies are calculated using the assumption that there is perfect contact between bearing components. Possibly due to distortion of the test bearing components under the high loading, the outer race bearing fault frequency was higher than the theoretical value, which was 587.0 Hz.

CUMULATIVE RUN TIME	AXIAL LOAD
0.0 - 16.6 hours	4.5 kN
16.6 - 29.1 hours	6.6 kN
29.1 - 41.25 hours	9.0 kN

Bearing failed on the outer race after 41.2 hours of run time.

4.2 Test 2

The second test bearing was run with an axial load of 9.0 kN which was maintained throughout the test at a rotational speed of 100 Hz. The recording of the vibration signal was performed on the Racal recorder using a continuous sequence mode at a lower tape speed of 3.75 inches per second, enabling the entire vibration history of the bearing to be stored on two cassettes, with a bandwidth of 0 - 12.5 kHz.

The continuous sequencing facility on the Racal recorder enables channels one and five (vibration signal and tacho signal) to be recorded for the length of the tape, automatically incrementing the channels and reversing the direction of tape play at each end of the tape. This permits up to four channels of continuous recording time with brief interruptions at tape beginnings and ends, and also at cassette changes.

The bearing failed on the outer race after 5.8 hours of operation at 9.0 kN axial load. The type of failure was very similar to that of the previous test.

Analysis of the frequency spectrum of the enveloped signal showed clearly the onset and progression of the fault. The onset of the fault was indicated by the sudden appearance of sidebands of the ORBP frequency, and the sudden increase in amplitude of the peak at the ORBP frequency (Note that there is a peak at the ORBP frequency for a healthy bearing). Progression of the fault was indicated by the incremental increases in amplitude of the ORBP frequency peak and its sidebands as the fault enlarged during continued operation.

Summary of Test 2.

Inner Race Speed : 100 Hz ; tape recording frequency range : 0 - 12.5 kHz

Outer Race Ball Pass fault frequency : measured at 595.7 Hz

CUMULATIVE RUN TIME	AXIAL LOAD
0.0 - 5.9 hours	9.0 kN

Bearing failed on the outer race after 5.8 hours run time, after which the test continued for another 0.1 hours.

After completion of the second bearing failure test, modifications were made to the lubrication and cooling system of the bearing test rig. These modifications were made to improve oil flow and reduce the possibility of the test bearings failing due to factors other than fatigue, such as overheating.

In order to determine whether an even clearer indication of fault progression was possible using frequency bands higher than 0 - 12.5 kHz, it was decided to perform a third test with increased tape speed. The higher tape speed chosen needed to balance the effect of providing a higher frequency bandwidth for the envelope detector to filter, with the problem of increasing the quantity of recorded data as encountered in the first test.

4.3 Test 3

The third test bearing was run with an initial axial load of 9.0 kN which was maintained throughout the test at a rotational speed of 100 Hz. The recording of the vibration signal was performed on the Racal recorder using the continuous sequence mode (as described in the Test 2 results) at an intermediate tape speed of 7.5 inches per second using the IRIG wide band two standard, providing a frequency bandwidth of 0 - 25.0 kHz.

At this tape speed, each recording tape would be able to store 1.5 hours of continuous vibration signal. Since the area of interest for the purpose of this study is the vibration signal from the bearing before, during, and after failure, an estimate of the time to failure of the test bearing would have enabled efficient use of limited a limited number of recording tapes.

However, experimental tests performed by bearing manufacturers such as NSK [3] have demonstrated that the time to failure of populations of identical rolling element

bearings operating under identical conditions covers a very wide distribution. This is due to the fact that the failure mechanism of the bearing material due to fatigue is itself subject to dispersion. This meant that even a reasonable prediction of the time to failure of a single bearing was not possible.

To reduce the number of cassettes used to record the vibration history of the test bearing, the decision was made to hold only three hours of vibration record at any time by reusing tapes cyclically. This procedure was changed to continuous recording after a change in the vibration signal occurred, thus providing a vibration history that began 4.5 hours before the fault occurred, right through fault development and up to well after the fault was fully developed. The detection of a change in the vibration signal was a subjective process based on the unfiltered vibration signal displayed on the CRO. This procedure was justified by the observation that there was very little change in the vibration signals of a bearing preceding the sharp increase at failure.

A change was observed in the unfiltered vibration signal after approximately 16.0 hours of run time, prompting the replacement of the tape recycling procedure with the conventional continuous recording. The bearing failed suddenly after 22.2 hours of run time, exhibiting a significant sudden increase in the amplitude of the ORBP frequency peak and subsequent sharp increases in amplitude as the fault increased in severity. The form of the failure development and progression was very similar to that displayed by the first and second test bearings, but test bearing three demonstrated a slower fault progression than bearing two, possibly due to the increased oil flow and decreased operating temperature. Visual inspection showed a failure pattern on the outer race very similar to those of the previous tests.

Summary of Test 3.

Inner Race Speed : 100 Hz ; tape recording frequency range : 0 - 25.0 kHz

Outer Race Ball Pass fault frequency : measured at 595.7 Hz

CUMULATIVE RUN TIME	AXIAL LOAD
0.0 - 24.2 hours	9.0 kN

Bearing failed on the outer race after 22.2 hours of run time, after which the test ran on for an additional 2.0 hours.

5. RESULTS AND DISCUSSION

The vibration records generated by the test bearings were analysed first with the digital method of envelope detection starting at the beginning of the history and sampling at irregular intervals up until immediately before the onset of failure, and then at small, regular intervals throughout the progression of the fault. The acceleration level at the ORBP frequency, the Racal tape recorder counter reading, and the centre frequency were recorded.

The analysis was then repeated using the Bruel and Kjaer WB1048 envelope detector in conjunction with the Bruel and Kjaer 2034 Signal Analyser. Twenty averages of the spectrum of the envelope were calculated at points in the vibration history corresponding to those points analysed with the digital algorithms, and measurements of the acceleration level at the ORBP frequency were made and recorded.

The level of the fundamental fault frequency generated by both analyses for each test was plotted on a single graph of Acceleration (G's) verses Run time (hours). It can be seen from figure 11a that the absolute amplitudes of the digital results are approximately eight times the amplitudes of the analogue results. This is due to the fact that the analogue values are related to the amplitude of the modulated frequency times the amplitude of the modulation frequency (see appendix A), whereas the digital algorithm produces a value based on the modulation amplitude only, as outlined in section 3.2. However, the usefulness of a fault detection method is defined by its ability to register a change in the characteristic conditions, not by the magnitude of the output of the measuring device. Standardisation of the results was achieved by calculating the mean and standard deviation of the fundamental fault frequency levels for the run time preceding the onset of failure. Each datum was then plotted as a multiple of the standard deviation from the mean level. Performing this procedure on both the analogue and digital results for each test allows the direct comparison of the standardised results. This method of representation allows the employment of vibration warning levels that have a degree of consistency from machine to machine.

Presentation of the same results using a statistical ordinate axis as a method of standardising the two sets of results demonstrates the similarity in the fault progression detected by the two methods. Figure 11b shows the standardised data from each test.

It was also observed that the sudden onset of failure in each test was clearly announced by sudden increases in the overall RMS level and also the sudden appearance of sidebands of the fundamental fault frequency in the raw vibration spectrum, both indicators less sophisticated than envelope analysis. This does not indicate that envelope analysis is redundant. The idealised environment of the laboratory enabled the observation of these two phenomena at the onset of failure that would have gone unnoticed with the background noise and adjacent machinery present on a plant or factory floor.

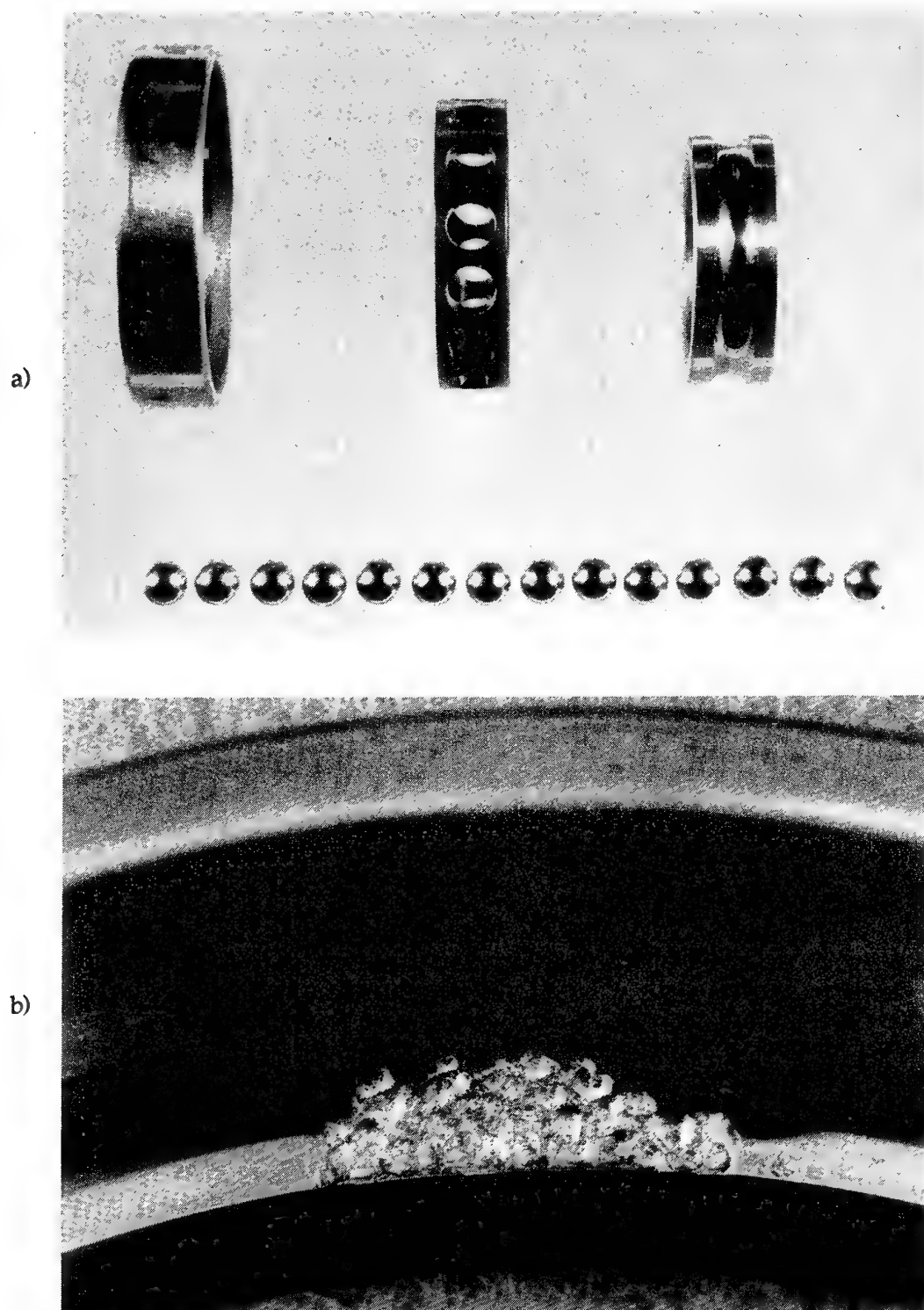


Figure 10. a) Disassembled NSK 7006C Angular Contact Bearing. b) Outer Race Failure.

These results indicate that the analogue envelope detection system is especially useful for continuous real time measurement of vibration signals from small systems, or for obtaining quick readings from any station on a large system. In its present configuration, the results obtained from the analogue envelope detector need to be entered manually onto a database, thus restricting the number of measurement points contained in the database to modest proportions. However, PC-based application software packages such as that provided by Bruel and Kjaer do exist that enable fast electronic access to computer-stored databases, permitting the application of analogue envelope detection techniques to any size system.

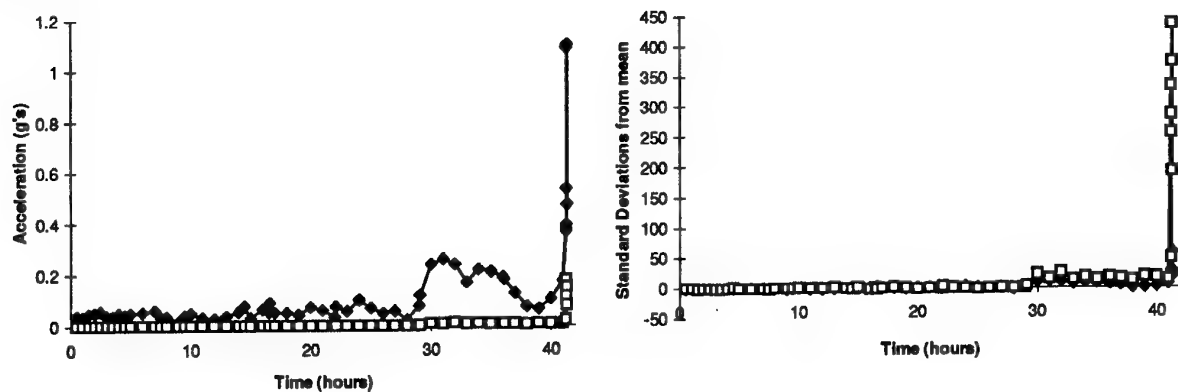
It was found that an accurate reading of the peak at the ORBP fault frequency with the analogue envelope detector was available in real time, while in addition producing an instantaneous spectrum of the envelope that was updated twice every second. In contrast, the time taken by the digital algorithms to produce the same product was approximately seven minutes, due to the large number of computations and dependent on the processing speed of the Personal Computer.

It appears that the digital envelope detection algorithms are more suitable for large scale monitoring programs which have a large number of measurement points and other variables, due to the fast and ready electronic access to a potentially very complex database. Such monitoring systems are advantageous for long term projects, and include additional machine condition trending and warning capabilities. The analysis algorithms may also be easily modified to accommodate different digital filter shapes, bandwidths, and so on.

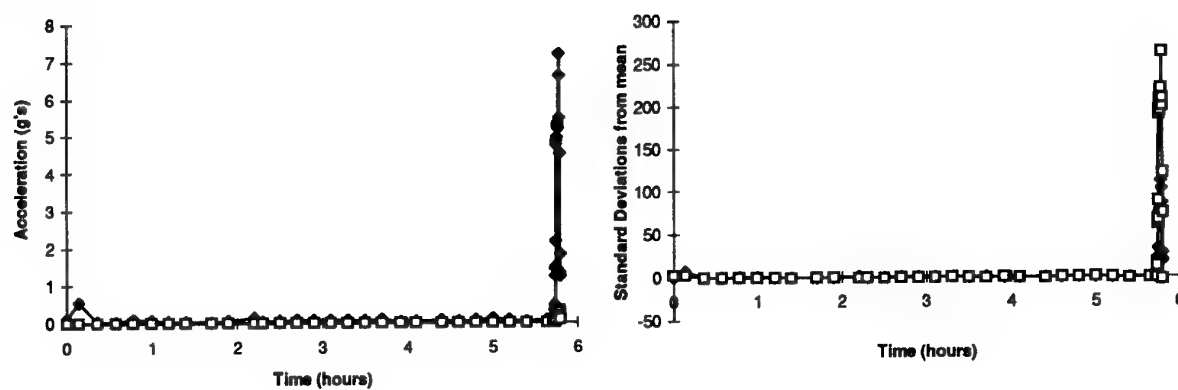
The time histories of the fault progression indicate that the severity of the fault-induced vibration fluctuates quite markedly as shown in figure 12. A suggested hypothesis for explaining this behaviour is that the fault progresses in a stepping fashion, as follows:

1. Bearing running smoothly.
2. Pit, or spall, in outer race occurs, causing immediate sharp increase in the spectrum of the vibration signal envelope, due to the sharp nature of the edges of the spall.
3. Rounding of the spall occurs as a result of continuous impacts from rolling elements, causing the impacts to lessen in severity and reduce the spectrum of the vibration signal envelope.
4. Further spalling occurs causing immediate sharp increase in the spectrum of the vibration signal envelope, again due to the sharp nature of the edges of the new spall. Successive rounding and spalling could account for the fluctuating vibration levels, and produce the observed outer race fault. See figure 10b).

Test 1.



Test 2.



Test 3.

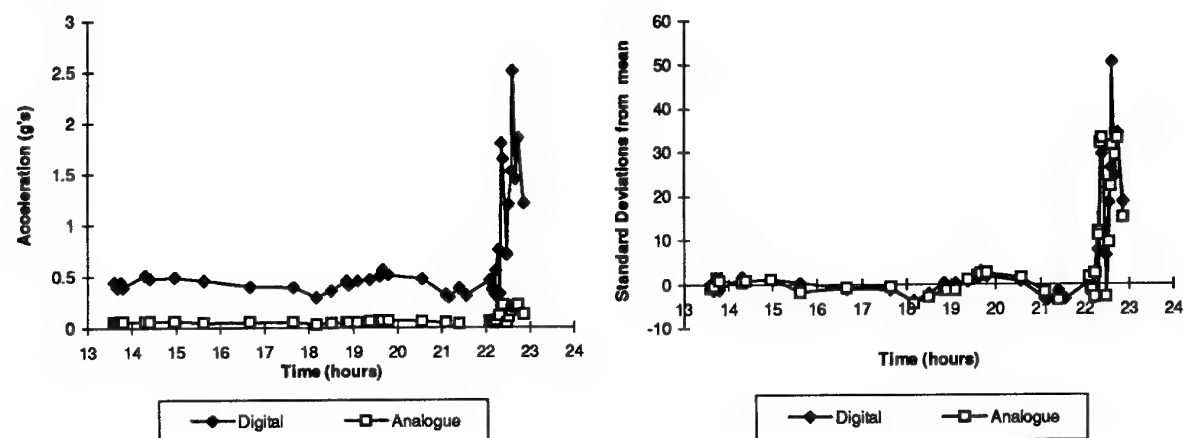


Figure 11. a) Raw results.

b) Standardised results

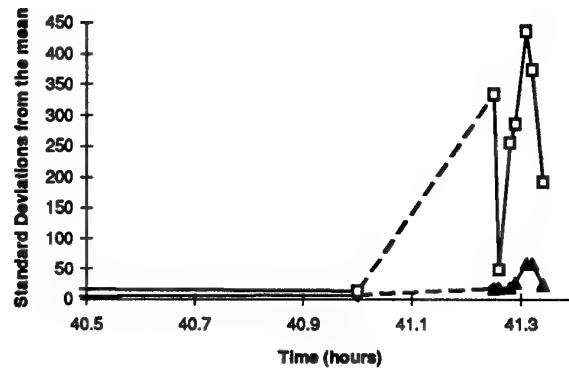
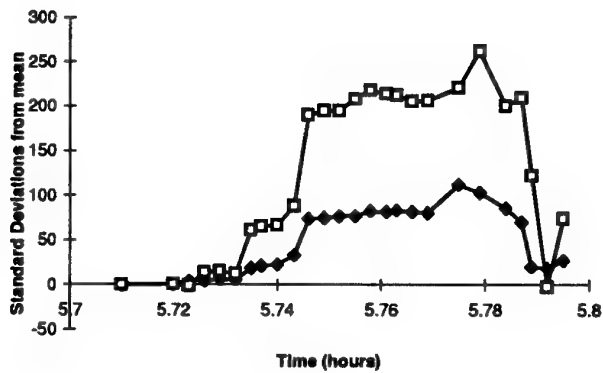
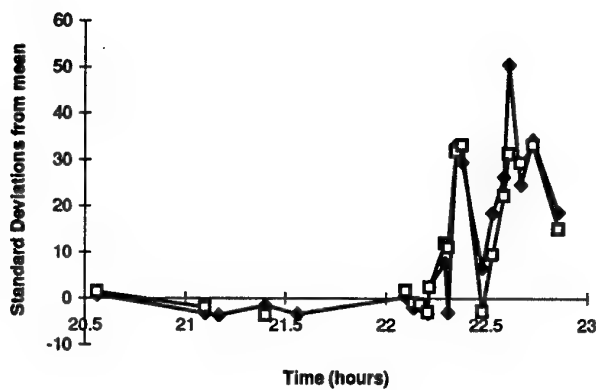
Test 1.**Test 2.****Test 3.**

Figure 12. Progression of bearing failure of tests 1, 2, and 3.

6. CONCLUSIONS

There is no significant advantage in terms of detection performance derived from using the digital envelope detection method above the analogue method. Both methods were able to detect the onset of failure at the same point in each bearing's time history.

However, each method of envelope detection method displayed other characteristic advantages and disadvantages:

SPEED OF RESULT	ANALOGUE Real time	DIGITAL Slow (~7.0 minutes) Dependent on processor speed.
ACCESSIBILITY OF RESULT	Manual entry of result onto modest database, perhaps an ongoing graph.	Automatic entry of result onto a potentially very large database, with information retrieval limited only by computer processing speed.
RECOMMENDED USAGE	Anything needing a quick result, or on small systems. Short or long term.	Large complex systems with long term condition monitoring.

Table 1. Comparison of Analogue and Digital envelope detection methods

7. REFERENCES

1. Application of Vibration Analysis to the Condition Monitoring of Rolling Element Bearings ; N.S. Swansson, S.C. Favoloro ; Aero Propulsion Report 163, AMRL, Melbourne. 1984
2. Vibration Analysis for Bearing Fault Detection; I.M. Howard, Y.Y. Link; Proceedings of the 1991 Asia-Pacific Vibration Conference, Volume 1.
3. NSK Ball and Roller Bearings; 1979
4. Bruel&Kjaer Envelope Detector WB1048 Instruction Manual 1986
5. Bruel&Kjaer Dual Channel Signal Analyser Type 2034 Instruction Manual 1983
6. SKF General Catalogue. SKF 1970

8. ACKNOWLEDGMENTS

The valuable technical support and advice offered by David Forrester, Brian Rebbechi, and Ken Vaughan is gratefully acknowledged.

APPENDIX A.

How Rectification of Analogue Signal Reveals Fundamental Fault Frequency.

The band pass filtered signal is rectified by a full wave rectifier:

For a signal $s(t) = A \cos(\omega_1 t)$,

Full wave rectified, the signal $s(t)$ becomes $s_r(t) = \text{abs}(A \cos(\omega_1 t))$.

The Fourier series of the rectified signal is as follows:

$$s_r(t) = \frac{2A}{\pi} + \sum_{n=1}^{\infty} \frac{4A(-1)^n}{\pi(1-4n^2)} \cos(2\omega_1 nt),$$

where $\frac{2A}{\pi}$ is the DC offset,

and n is an integer between 1 and infinity.

If the rectified signal $s_r(t)$ was modulated by the modulation signal $m(t) = (C + M \cos(\omega_2 t))$

where M is the amplitude of the modulation frequency ω_2 , and C is some DC offset, then the modulated signal $s_m(t) = m(t)s_r(t)$ becomes:

$$s_m(t) = (C + M \cos(\omega_2 t)) \left(\frac{2A}{\pi} + \sum_{n=1}^{\infty} \frac{4A(-1)^n}{\pi(1-4n^2)} \cos(2\omega_1 nt) \right).$$

This contains the component $\frac{2MA}{\pi} \cos(\omega_2 t)$, which is a cosine at the modulation

(fault) frequency ω_2 , with amplitude $\frac{2MA}{\pi}$. Note that the amplitude of the

component at the fault frequency is directly proportional to the amplitude of the modulated frequency and the amplitude of the modulation frequency. In this simplified example of a single carrier frequency at ω_1 modulated by a single

modulation frequency at ω_2 , the amplitude seen at ω_2 would be $\frac{2MA}{\pi}$. In real

data, many frequencies are represented, making the actual the amplitude seen at ω_2 difficult to interpret. Note that the value generated by digital methods should be the actual modulation value V , or V^2 for a squared envelope.

APPENDIX B.

Power Supply and Interface Circuit for the Bruel and Kjaer WB1048 Envelope Detector.

The Bruel and Kjaer WB1048 envelope detector was designed to be used in conjunction with the Bruel and Kjaer 2515 Signal Analyser. To make the device compatible with existing equipment, an interface and power supply module that emulated the input and output functions of the 2515 Signal Analyser was built. Reference to the supplied circuit diagrams provided information about the pin functions on the socket of the envelope detector. The pin layout is shown in figure B1.

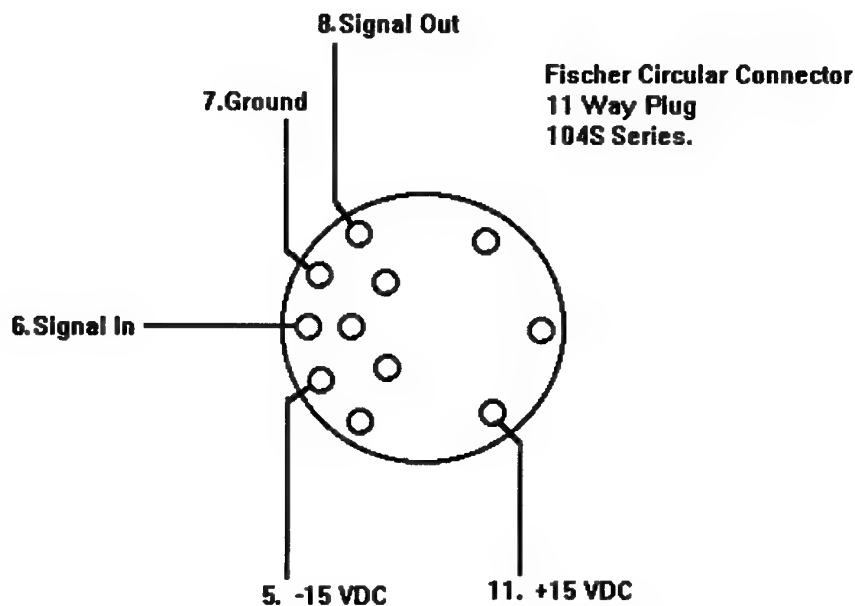


Figure B1. Envelope detector Connector Plug Pin Functions.

Four nine-volt batteries were used to provide a $\pm 18V$ supply voltage, with the option of an external power supply in the event of low battery voltage. Input and output are provided by standard BNC jacks. The final circuit for the interface unit is shown in figure B2.

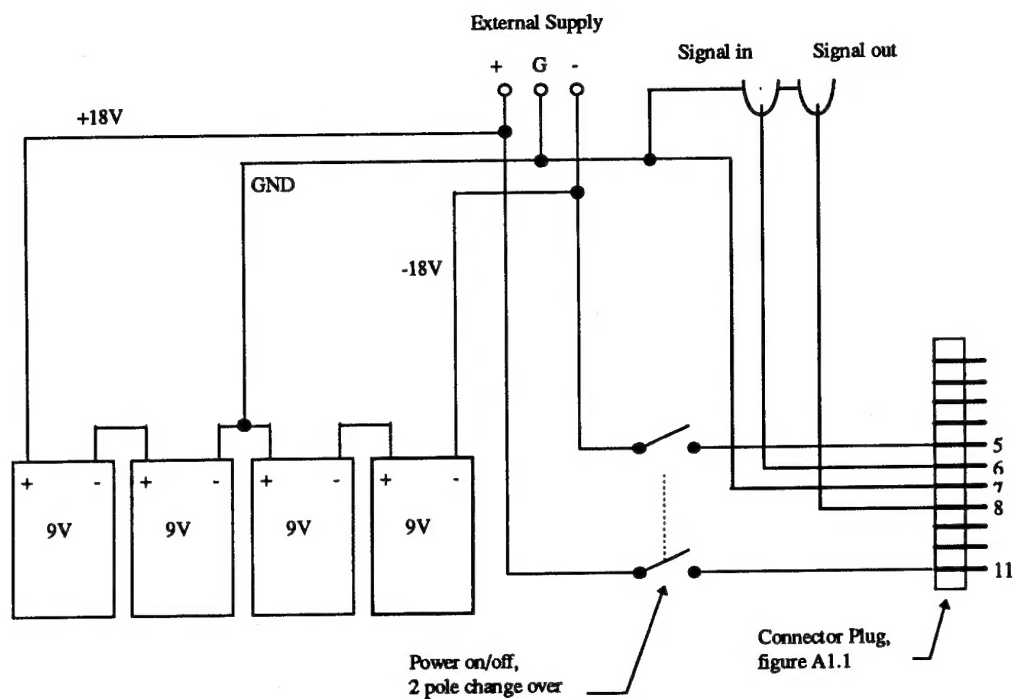


Figure B2. Battery Supply and Input/Output Circuit for envelope detector.

The components were mounted in a standard 3cm x 6cm x 11cm project box and used in conjunction with the Bruel and Kjaer type 2034 Signal Analyser and the Bruel and Kjaer WB1048 envelope detector for the analysis of the vibration records made from the Ball Bearing tests.

**A Comparison of Digital and Analogue Vibration Analysis Techniques for the
Detection of Ball-Bearing Faults**

Mark Shilo

AUSTRALIA

DEFENCE ORGANISATION

Defence Science and Technology Organisation

Chief Defence Scientist	}	shared copy
FAS Science Policy		
AS Science Corporate Management		
AS Science Industry Interaction		
Counsellor Defence Science, London (Doc Data Sheet only)		
Counsellor Defence Science, Washington		
Scientific Adviser to Thailand MRD (Doc Data Sheet Only)		
Scientific Adviser to the DRC (Kuala Lumpur) (Doc Data Sheet Only)		
Senior Defence Scientific Adviser/Scientific Adviser Policy and Command (shared copy)		
Navy Scientific Adviser (3 copies Doc Data Sheet and one copy of the distribution list)		
Scientific Adviser - Army (Doc Data Sheet and distribution list)		
Air Force Scientific Adviser		
Director Trials		

Aeronautical and Maritime Research Laboratory

Director AMRL
Chief Airframes and Engines Division
S. Fisher
Author: Mark Shilo
D.M. Blunt
M. Burchill
B.D. Forrester
B. Rebbechi
C. Vavlitis

DSTO Library

Library Fishermens Bend
Library Maribyrnong
Library DSTOS (2 copies)
Library, MOD, Pyrmont (Doc Data sheet)

Defence Central

OIC TRS, Defence Central Library
Officer in Charge, Document Exchange Centre (DEC), 8 copies
Defence Intelligence Organisation
Library, Defence Signals Directorate (Doc Data Sheet only)

Air Force

TASK SPONSOR: DTA-LSA
OIC ATF ATS, RAAFSTT, WAGGA (2 copies of all unclassified RAAF
sponsored documents)

Army

Director General Force Development (Land), (Doc Data Sheet only)
ABCA Office, G-1-34, Russell Offices, Canberra (4 copies)

UNIVERSITIES AND COLLEGES

Australian Defence Force Academy
Library
Head of Aerospace and Mechanical Engineering
Senior Librarian, Hargrave Library, Monash University

OTHER ORGANISATIONS

NASA (Canberra) (Doc Data Sheet only, if document limited to Australia)
AGPS (Public Release only)

ABSTRACTING AND INFORMATION ORGANISATIONS

INSPEC: Acquisitions Section Institution of Electrical Engineers
Library, Chemical Abstracts Reference Service
Engineering Societies Library, US
American Society for Metals
Documents Librarian, The Center for Research Libraries, US

INFORMATION EXCHANGE AGREEMENT PARTNERS

Acquisitions Unit, Science Reference and Information Service, UK
Library - Exchange Desk, National Institute of Standards and
Technology, US
National Aerospace Laboratory, Japan
National Aerospace Laboratory, Netherlands

SPARES (Normally 10 copies)

DEFENCE SCIENCE AND TECHNOLOGY ORGANISATION DOCUMENT CONTROL DATA				1. PRIVACY MARKING/CAVEAT (OF DOCUMENT)	
2. TITLE A comparison of digital and analogue vibration analysis techniques for the detection of ball bearing faults			3. SECURITY CLASSIFICATION (FOR UNCLASSIFIED REPORTS THAT ARE LIMITED RELEASE USE (L) NEXT TO DOCUMENT CLASSIFICATION) Document (U) Title (U) Abstract (U)		
4. AUTHOR(S) Mark Shilo			5. CORPORATE AUTHOR Aeronautical and Maritime Research Laboratory PO Box 4331 Melbourne Vic 3001		
6a. DSTO NUMBER DSTO-TN-0024		6b. AR NUMBER AR-007-998		6c. TYPE OF REPORT Technical Note	
				7. DOCUMENT DATE January 1996	
8. FILE NUMBER M1/9/123	9. TASK NUMBER 20238B	10. TASK SPONSOR DTA-LSA	11. NO. OF PAGES 22	12. NO. OF REFERENCES 5	
13. DOWNGRADING/DELIMITING INSTRUCTIONS			14. RELEASE AUTHORITY Chief, Airframes and Engines Division		
15. SECONDARY RELEASE STATEMENT OF THIS DOCUMENT <p style="text-align: center;">Approved for public release</p> OVERSEAS ENQUIRIES OUTSIDE STATED LIMITATIONS SHOULD BE REFERRED THROUGH DOCUMENT EXCHANGE CENTRE, DIS NETWORK OFFICE, DEPT OF DEFENCE, CAMPBELL PARK OFFICES, CANBERRA ACT 2600					
16. DELIBERATE ANNOUNCEMENT <p style="text-align: center;">No limitations</p>					
17. CASUAL ANNOUNCEMENT Yes					
18. DEFTTEST DESCRIPTORS Vibration measurement, Ball bearings, Detection, Condition monitoring, Signal analysis, Fourier transformation					
19. ABSTRACT A comparison of Digital and Analogue Envelope Detection techniques was performed on the vibration signals generated by the failure of three NSK type 7006C angular contact bearings to determine the relative merits of each technique.					